S-BAND PHOTOCATHODE GUN WITH A 1 kHz REPETITION RATE

J.-H. Han, D. Brice, M. Cox, H. Huang, S. Pande, Diamond Light Source, Oxfordshire, UK

Abstract

Photocathode RF guns have been developed in many labs to generate high quality beams for free electron lasers and linear colliders. Recently such guns are also used as electron sources for ultrafast electron diffraction and *x*/γ-ray radiation through Compton scattering. Normal conducting guns generate very low emittance and short pulse electron beams thanks to their high accelerating field and the possibility of optimum focusing solenoid positioning. They are however generally limited in repetition rate to 100-120 Hz. Here, we report our activity on the design and production of an S-band normal conducting photocathode gun for a 1 kHz repetition rate. The RF characteristics, RF heating, and vacuum analyses are discussed.

INTRODUCTION

At Diamond Light Source, an S-band (2998 MHz) normal conducting gun had been designed for improved beam parameters and a high repetition rate operation [1]. In that gun design, a coaxial RF coupler was adopted as at the DESY gun [2]. With the coaxial coupler, the coupling is made at the region where the RF power dissipation is low. Therefore, the coupling region does not limit the repetition rate in terms of the temperature rise and the corresponding body stress. The coaxial coupler also allows axisymmetric cooling-water channel installation around the cavity cylinder so that cooling capacity can be maximal and the cavity deformation due to RF heating is also axisymmetric. A gun main solenoid should be placed around the gun second cell to achieve a minimum transverse emittance [2, 3] by the so-called emittance compensation process [4]. The focusing solenoid can be placed at such a position when a coaxial coupler is used. High order transverse RF modes can be eliminated due to the perfectly symmetric cavity inner surface.

In the present design, further improvements have been made for an exchangeable cathode, cooling-water channels, and elliptic irises (see Fig. 1). The first step was to include a cathode slot at the rear wall of the gun. With the cathode slot, photocathodes can be exchanged and various emitting materials such as Cu, Mo, or Cs-Te can be tested. The cooling-water channels were improved for uniform temperature distribution over the gun body as well as a higher cooling capacity and for the mechanical sustainability with a high water pressure. The elliptic shape irises allow a lower surface field. The gun section layout including the focusing solenoids is shown in Fig 1.

In this paper, we report the RF design, thermal analysis, and vacuum simulation of the new gun, which will be produced with oxygen-free electronic (OFE) copper. A prototype of the gun was produced for low power RF tests with a network analyzer. The test results with the prototype are also discussed.

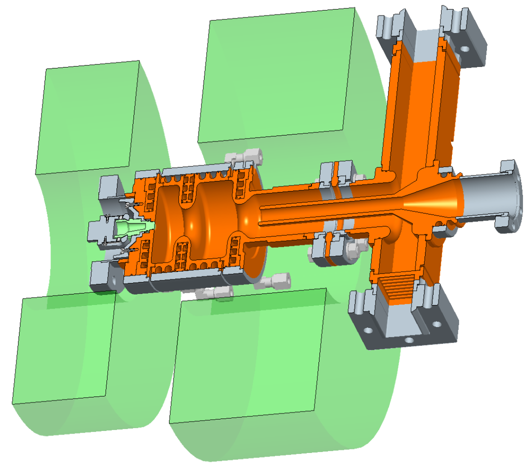

Figure 1: Gun section layout. It consists of a gun and a coupler. An exchangeable cathode is installed at the rear wall of the gun. The connecting parts to other vacuum components and RF window are shown. The focusing solenoids are also shown.

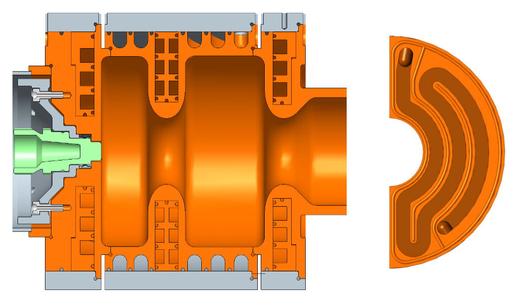

Figure 2: A cut view of the gun body (left) and a half of the cooling channel in the irises and rear wall (right). There are 8 water inlets and 8 outlets in total.

RF DESIGN

The gun RF design was carried out with SUPERFISH [5]. The lengths of the first and second cells were chosen to 0.28 and 0.5 of the resonance wavelength (0.1 m) after beam dynamics optimization [1, 6]. The field at the first cell is higher than at the second cell by 5% for uniform dissipated RF power density at both the cells. The details such as the cathode plug and the slot for the plug at the rear wall of the gun as well as the coupler antenna in front of the gun were included in the RF simulation. The quality factor is 13700 at 45°C. The separation between two resonant modes, π and 0-modes, is 21 MHz.

The RF coupler was designed with CST Studio [7]. The coaxial coupler tube was designed to be long enough to place the main focusing solenoid around the second cell of the gun. Then, the coaxial part was tuned to minimize the RF reflection. The gap between the end tip of the coupler inner antenna and the iris of the gun cavity front opening was optimized for a critical RF coupling.

THERMAL ANALYSIS

A peak RF power of 5.6 MW is required to achieve a 100 MV/m amplitude at the cathode when the gun operates at 45°C. When this gun operates with a 3 μs RF pulse length and a 1 kHz repetition rate, the average power is 17 kW. The RF power dissipation calculated with SUPERFISH was used for the steady state temperature, deformation, and stress analyses with ANSYS [8]. For these analyses, a cooling-water temperature of 20°C and a flow rate of 4 m/s were used. The maximum temperature at the gun is 47°C, which appears at the iris (Fig. 3). The cavity deformation was analyzed with the temperature distribution. The left end flange was fixed for the analysis. The maximum deformation is about 40 μm (Fig. 4).

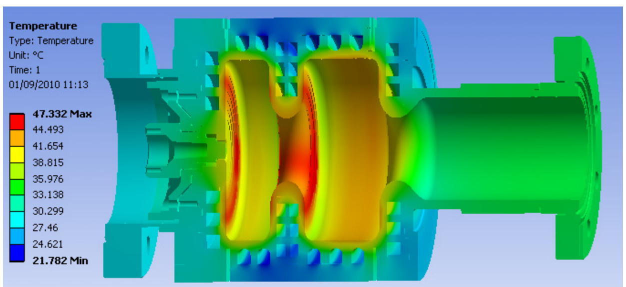

Figure 3: Temperature distribution at the steady state.

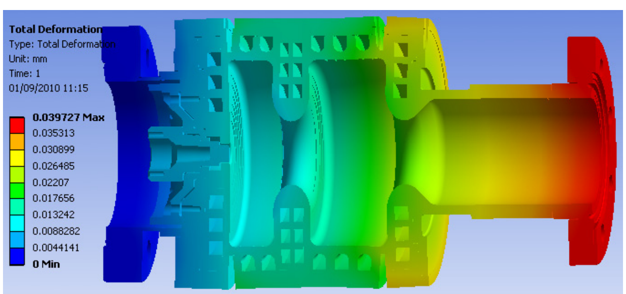

Figure 4: Cavity deformation caused by the RF heating.

The local stress caused by the RF heating should be controlled below the yield stress of the annealed oxygen-free copper, 62 MPa [9]. At the corner of the second cell the stress is 45 MPa (Fig. 5), which is marginal but in the safe region. The stress at the cathode plug is below 15 MPa (not shown).

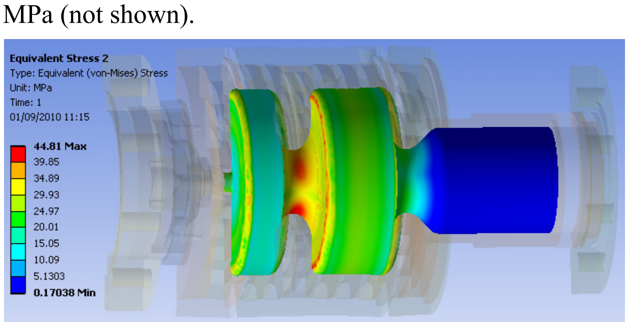

Figure 5: Steady state von Mises stress on the RF surface of the copper body.

The surface temperature rise, ΔT_s, by RF pulse heating can be found with the equation [10]:

$$\Delta T_s = \frac{2 P_{RF} \sqrt{\tau}}{\sqrt{\pi \rho k C_\varepsilon}},$$

where P_{RF} is the dissipated RF power density, and τ is the pulse length. $\rho = 8.93 \times 10^3$ kg/m^3, $k = 391$ W/m·K and $C_\varepsilon = 385$ J/kg·K are the material density, the heat capacity and the specific heat for the OFE copper. A maximum dissipation of 225 MW/m^2 occurs at the iris. For 100 MV/m and 3 μs, the temperature rise is 12°C, which is far below the damage threshold for cyclic stress [9].

For the steady state condition, RF heat dissipation at the coupler was calculated with CST Studio and used for an ANSYS analysis. One turn of cooling-water channel was accommodated downstream of the inner antenna. A water temperature of 20°C and a flow rate of 2 m/s were used for this coupler cooling. The maximum temperature is 61.5°C (Fig. 6a). The deformation is about 60 μm (Fig. 6b) but the impact on the RF coupling is negligible. The maximum von Mises stress is 1.6 MPa (Fig. 6c).

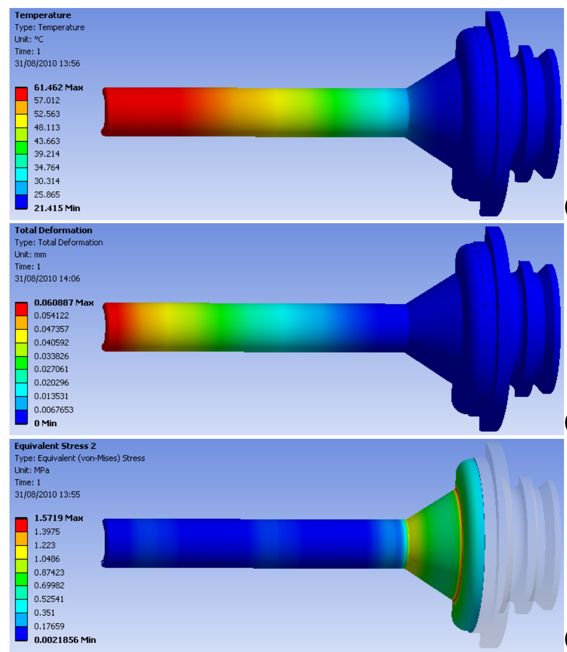

(a)
(b)
(c)

Figure 6: Steady state temperature (a), deformation (b), and stress (c) at the coupler inner antenna.

VACUUM SIMULATION

There is no pumping port connected directly to the gun body: pumping is achieved through the RF coupler and the downstream beam pipe. At one end of the coupler waveguide there is an RF shielding grill to reflect the RF wave with parallel slots allowing pumping to ultra-high vacuum by a 100 l/s ion pump (see Fig. 1 and Fig. 7a). In the vacuum simulation, additional pumping is provided with a second 100 l/s ion pump at the downstream beam pipe as a simplified representation of the final design. At the other end of the rectangular waveguide connected to the coupler, an RF window will be installed. Near the window, small additional pumps will be installed; these are not shown in Fig. 7a and were omitted from the vacuum simulation.

The pressure distribution was simulated using the Monte-Carlo Test Particle software, MCTPVac [11], developed in-house. An outgassing rate of 10^{-11} mbar l/s·cm^2 at the vacuum surface, which should be achieved after full RF conditioning, and a gas molecular mass of 28 (nitrogen equivalent) were assumed. The highest calculated pressure is found in the first cell of the gun but stays below 8×10^{-10} mbar (Fig. 7b).

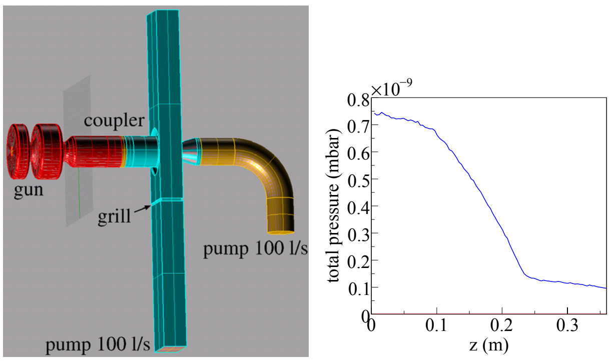

(a) Vacuum surface model. (b) Pressure in the gun.

Figure 7: Vacuum simulation. The simulation shows the total pressure on the symmetry axis of the gun. The cathode is at z = 0.

COLD TEST WITH A PROTOTYPE

A simplified prototype was produced to test the RF characteristic with a network analyzer (Fig. 8). The body material was a low grade oxygen-free copper. The machining tolerance and surface finishing were relaxed to reduce the production cost. The machined parts were vacuum brazed. The measured S11 parameters for 0- and π-modes are shown in Fig. 9. The RF parameters are summarized in Table 1.

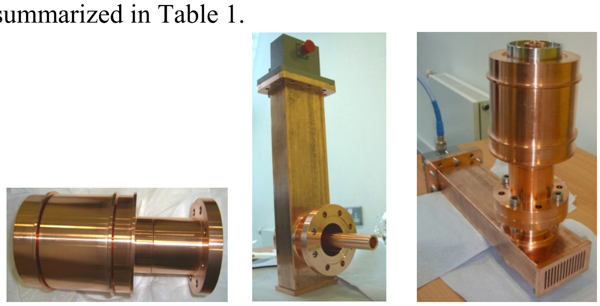

(a) Gun. (b) Coupler. (c) Gun + coupler.

Figure 8: Constructed prototype for cold test.

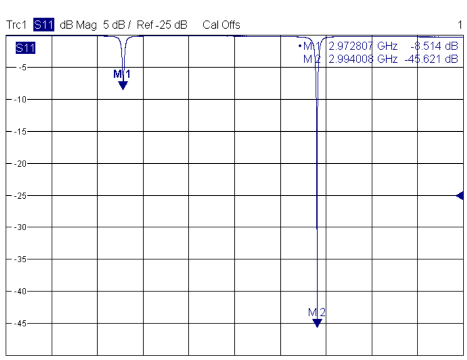

Figure 9: S11 measurement with a network analyzer.

Table 1: Design Parameters and Measured Ones with the Prototype.

Parameters	Design	Prototype
$\beta_{\pi\text{-mode}}$	1	0.99
$f_{\pi\text{-mode}}$	2998	2994
$Q_{\pi\text{-mode}}$ at 25°C	13875	12280
field balance	1.04	1.02
Δf (π-0 mode)	20.8	21.2
$\beta_{0\text{-mode}}$		0.453
$Q_{0\text{-mode}}$ at 25°C	11870	10504

There were resonance frequency and quality factor differences between the designed and measured ones due to the relaxed machining. However, the RF coupling was very near to the critical coupling as designed.

RF tuning was practiced by using the plastic deformation of the rear and front walls as carried out for the DESY gun [12]. Tuning up to 400 kHz with the rear wall and 100 kHz with the front wall were achieved.

SUMMARY AND OUTLOOK

An S-band gun has been designed for a 1 kHz operation. A prototype was constructed and the RF characteristics were confirmed. Production of an operational gun is under preparation and a high power test is foreseen using the RF system of the Diamond Light Source injector linac [13]. Possible future applications with this gun are studied in [14, 15].

ACKNOWLEDGEMENTS

We thank N. Hammond, M. Jensen, J. Kay, A. Peach, and L. Zaja for their helps on the design. JHH thanks K. Floettmann at DESY for valuable discussions and G. Materlik and R. Walker for encouraging this study.

REFERENCES

[1] J.-H. Han, LINAC08, TUP099, p. 636.
[2] B. Dwersteg et al., Nucl. Instr. and Meth. A **393**, 93 (2997).
[3] R. Alley et al., Nucl. Instr. and Meth. A **429**, 324 (1999).
[4] B. E. Carlsten, Nucl. Instr. and Meth. A **285**, 313 (1989).
[5] J. H. Billen and L. M.Young, "Poisson Superfish", LAUR-96-1834.
[6] J.-H. Han, PAC09, MO6RFP059, to be published.
[7] CST Studio, http://www.cst.com.
[8] ANSYS, http://www.ansys.com.
[9] D. Pritzkau and R. H. Siemann, Phys. Rev. ST Accel. Beams **5**, 112002 (2002).
[10] D. Pritzkau, SLAC-R-577 (2001).
[11] B. F. Macdonald et al., Vacuum **84**, 283, 2009.
[12] S. Rimjaem et al., EPAC08, p. 244.
[13] C. Christou, Theses Proceedings, MOP017.
[14] J.-H. Han, These Proceedings, THP105.
[15] J.-H. Han, These Proceedings, THP106.